Tetrahedron 193 (2026) 135150

Contents lists available at ScienceDirect

Tetrahedron

journal homepage: www.elsevier.com/locate/tet

A novel progesterone product obtained by biooxidation from marine-derivated fungus *Penicillium oxalicum* CBMAI 1996

Ligia Breda e Vasconcelos [a], Samuel Filipe Cardoso de Paula [a], Pedro Henrique de Oliveira Santiago [b], Javier Ellena [b], André Luiz Meleiro Porto [a,*]

[a] *Laboratório de Química Orgânica e Biocatálise, Instituto de Química de São Carlos, Universidade de São Paulo, Av. João Dagnone, 1100, Ed. "Prof. Wagner Douglas Franco", J. Santa Angelina, São Carlos, SP, 13563-120, Brazil*

[b] *Laboratório Multiusuário de Cristalografia Estrutural, Instituto de Física de São Carlos, Universidade de São Paulo, Av. Trabalhador São-carlense, 400, Parque Arnold Schmidt, São Carlos, SP, 13566-590, Brazil*

ARTICLE INFO

Keywords:
Marine fungi
Progesterone
Biotrasnformation
Emerging contaminants
Hormones

ABSTRACT

- In this work, the green synthesis method based on the bio-oxidation of progesterone was investigated using the mycelium of the marine-origin fungus, *Penicillium oxalicum* CBMAI 1996. The structural characterization of a novel minor product, **2β,15β-dihydroxyprogesterone** (**2β,15β-di-OH**), was carried out using NMR techniques (1D, ^{1}H and ^{13}C; 2D, HSQC, HMBC, COSY, and NOESY), FTIR, and single crystal X-ray diffraction. The biotransformation reactions of progesterone to obtain the compound **2β,15β-di-OH** were carried out in quintuplicate over 15 days (32 °C, 130 rpm, pH 7.4). Furthermore, the novel X-ray single crystal analyses of the major products, **15β-hydroxyprogesterone** (**15β-OH**) and **7β,15β-dihydroxyprogesterone** (**7β,15β-di-OH**), which were also previously isolated from the fungus *P. oxalicum* CBMAI 1996, unequivocally confirmed their structural formulas. It was also possible to determine from the X-ray analyses the absolute configuration of the hydroxylated chiral carbons, so the obtained values were 15*R*–OH, 7*S*,15*R*-di-OH, and 2*S*,15*R*-di-OH.

1. Introduction

Steroids are biologically active molecules capable of interacting with high specificity with enzymes and receptors. Secreted by the adrenal cortex, testis, and ovaries in humans and other animals, these compounds play a pivotal role in various physiological processes. Progesterone, produced by the ovaries, is responsible for regulating steroid action in the female human body during the reproductive cycle [1,2]. Progestogens, one of the primary groups of endogenous steroids in humans, are characterized by molecules composed of 18 carbon atoms arranged in four fused rings, with carbonyl groups at C-3 and C-17 [3]. A diverse array of semi-synthetic derivatives of progesterone are produced and utilized in contraceptive pills.

In the human body, both natural and synthetic steroid hormones are metabolized and excreted in urine as glucuronides and sulfates [4]. Due to their lipophilic nature, high stability, and low concentrations (ranging from 0.1 to 439 ng L^{-1}), traditional wastewater treatment methods are often ineffective at removing them [5]. The growing concern over aquatic contamination by this class of compounds, which exhibit significant endocrine-disrupting potential, has prompted numerous studies in recent years [6].

Biotransformation refers to changes induced in xenobiotic molecules, used as reagents, by biological processes. Biotransformations lead to changes in the physicochemical properties of the products, which can be extracted and recovered after the reaction [7]. Biotransformation reactions can also result in subsequent biodegradation pathways of compounds. Due to the hydrophobic nature of steroids and a reduced number of functional groups, such substances are recalcitrant to biodegradation, in addition to having a high tendency for bioaccumulation in the environment. Thus, the importance of studying biotransformation and biodegradation reactions with microbial cells is understood, as these can also be naturally found in environments contaminated by steroids [8].

Studies conducted in the last 5 years have identified several species of fungi capable of promoting chemical alterations in the progesterone molecule. The filamentous fungus *Aspergillus nidulans* promoted the

This article is part of a special issue entitled: Brazil published in Tetrahedron.

* Corresponding author.
E-mail address: almporto@iqsc.usp.br (A.L. Meleiro Porto).

https://doi.org/10.1016/j.tet.2026.135150
Received 18 November 2025; Received in revised form 8 January 2026; Accepted 15 January 2026
Available online 21 January 2026

insertion of a hydroxyl group at carbon C-11, forming 11α-hydroxyprogesterone (240–250 rpm, 37 °C, 4 days). Furthermore, the formation of 6β,11α-dihydroxyprogesterone and 11α-acetoxyprogesterone was consecutively observed [9]. While the entomopathogenic filamentous fungus *Isaria farinosa* KCh KW1.1 converted progesterone into derivatives such as 17α-hydroxyprogesterone, 6β, 17α-dihydroxyprogesterone, 12β,17α-dihydroxyprogesterone, and 6β, 12β,17α-trihydroxyprogesterone (under orbital shaking at an unspecified speed, 25 °C, for 3 days) [10].

The endophytic fungus *Penicillium citrinum* H7, isolated from the leaf of *Handroanthus impetiginosus*, converted 93 % of progesterone into 17-methyltestosterone (25 °C, 120 rpm, 8 days) [11]. The fungi isolated from the marine environment, *Penicillium oxalicum* CBMAI 1996, *Mucor racemous* CBMAI 847, *Cladosporium* sp. CBMAI 1237, *Penicillium oxalicum* CBMAI 1185, and *Aspergillus sydowii* CBMAI 935, exhibited a progesterone conversion potential of 75–95 % within 24 h of reaction. With this, it became possible to isolate and characterize compounds such as testololactone, 12β-hydroxyandrostenedione, and 1β-hydroxyandrostenedione [12].

In previous studies on the bio-oxidation of progesterone, catalyzed by the marine fungus *Penicillium oxalicum* CBMAI 1996 in synthetic seawater (32 °C, 130 rpm, 14 days), the predominant products were the mono-hydroxylated compound 15β-hydroxyprogesterone (15β-OH) and the di-hydroxylated compound 7β,15β-dihydroxyprogesterone (7β,15β-di-OH) (Fig. 1). These findings underscore the significant oxidative capacity of the enzymatic system produced by *P. oxalicum* CBMAI 1996 in the biotransformation of progesterone [13].

The structural determination of steroids is a complex and crucial process, as even minor structural changes can significantly impact their biological function [14]. Consequently, it is important not only to discover new steroid derivatives through biotransformation processes but also to thoroughly characterize their structures. Modifications in functionalities and the identification of biodegradation pathways in steroids can offer potential for the development of new drugs and contribute to mitigating the environmental impacts of emerging contaminant molecules.

This study presents two novel investigations. The first involves the isolation and structural characterization of a minor product from the biotransformation of progesterone, 2β,15β-dihydroxyprogesterone (2β,15β-di-OH), produced by the fungus *P. oxalicum* CBMAI 1996 under the same experimental conditions previously employed by De Paula et al. [13]. The structural significance in the discovery of this new molecule lies in the hydroxylation site, at the C-2 position, which is uncommon in reported progesterone biotransformation. This finding reveals a distinctive regio- and stereoselective oxidative capability of the enzymatic system produced by the fungus.

The second study focuses on the complete structural characterization of the major products 7β,15β-di-OH and 15β-OH, also derived from *P. oxalicum* CBMAI 1996 [13] through the pioneering single-crystal X-ray analysis. Unique single crystals of these major biotransformation products were obtained after extensive purification of extracts derived from multiple reaction batches. These analyses enabled the confirmation of the relative structural assignments previously reported in the literature, as well as the unambiguous determination of the absolute configuration of the stereogenic centers at which hydroxylation occurred. Together, these findings provide robust structural data that are highly relevant for the understanding and future exploration of progesterone-derived scaffolds with potential pharmacological activity.

2. Results and discussion

2.1. Molecular characterization of 2β,15β-di-OH

The minor product **2β,15β-dihydroxyprogesterone,** isolated from the biotransformation of progesterone by the fungus *P. oxalicum* CBMAI 1996, was not found in various databases (PubMed, Web of Science, Scopus, ChemSpider, ChEMBL, ChemBank), suggesting that it is a novel hydroxylated derivative of progesterone. The proposed chemical structure of this minor compound is represented in Fig. 2. The carbon atoms were named according to the convention established jointly by the IUBMB (International Union of Biochemistry and Molecular Biology) and IUPAC (International Union of Pure and Applied Chemistry) [15]. The complete structural determination of the compound **2β,15β-di-OH** was achieved using GC-MS, FT-IR, NMR (1D and 2D), and single-crystal X-ray diffraction techniques.

2.2. Purification, analysis, and identification by CG-EM of the compound 2β,15β-di-OH

After the purification of the products from the progesterone biotransformation reaction by column liquid chromatography (**15β-OH** and **7β,15β-di-OH**) and TLC plate (**2β,15β-di-OH**), a sample was prepared for analysis by GC-MS (1 mg/mL), dissolved in ethyl acetate. Only the characterization data for the novel minor product (**2β,15β-di-OH**) are discussed here, as the major products **(15β-OH** and **7β,15β-di-OH**) had already been characterized by GC-MS, FT-IR, and NMR [13]. The peaks at retention times of 16.01 min and 16.44 min were attributed to the products **15β-OH** and **7β,15β-di-OH**, respectively, due to their matching chromatographic profiles observed in the study by de Paula et al. [13] and by comparison with samples of the isolated products.

This sample was then subjected to separation by semi-preparative thin-layer chromatography (TLC) for the isolation of the minor product **2β,15β-di-OH**. The chromatogram in Fig. 3 refers to the fraction obtained during the column chromatography purification step, with the peak at a retention time of 15.06 min corresponding to the minor product **2β,15β-di-OH**. The mass spectrum obtained for this analysis, corresponding to the peak of the compound **2β,15β-di-OH**, is shown in the supplementary material (SM-S1). According to the equipment's library (MS/NIST21 Library), the compound found with the highest similarity (61 %) was Androstan-17-one, 3,11-bis(formyloxy)-(3,α,5α,11β) (**SM-S2**).

The fraction obtained from the crude extract (2.3 g) by column

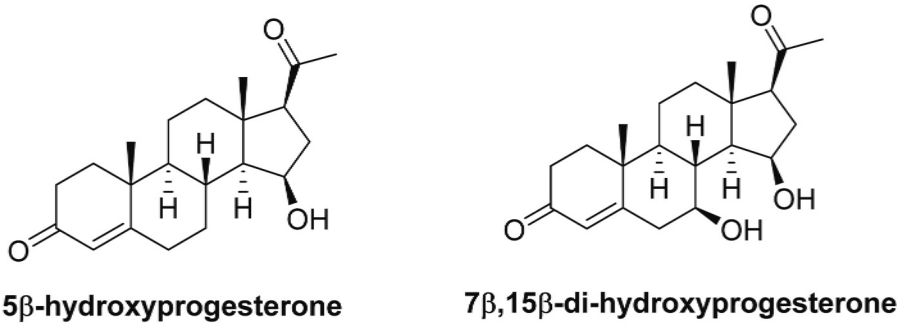

Fig. 1. Chemical structures of the hydroxylated products from the biotransformation of progesterone by the fungus *P. oxalicum* CBMAI 1996 (De Paula et al., 2021).

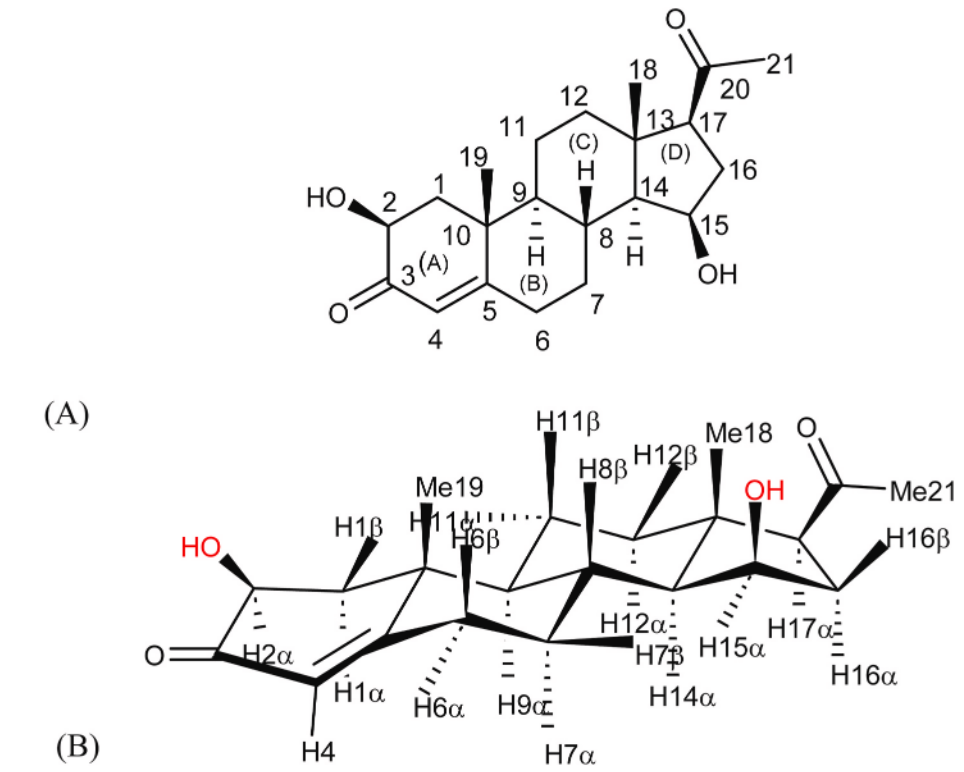

Fig. 2. Molecular structure of **2β,15β-dihydroxyprogesterone** (**2β,15β-di-OH**) obtained from the biotransformation of progesterone by the fungus *P. oxalicum* CBMAI 1996. (A) Planar structure with numbered carbon atoms. (B) Three-dimensional structure with numbered hydrogen atoms.

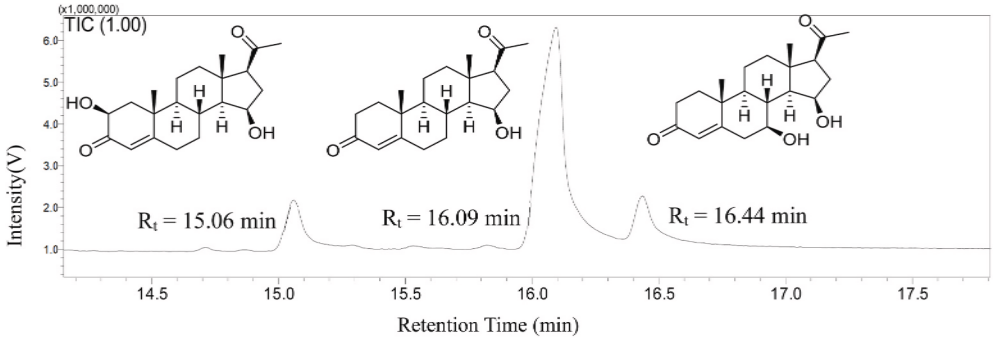

Fig. 3. Chromatogram obtained by GC-MS (EI, 70 eV) of the fraction obtained after column chromatography purification containing the compound **2β,15β-di-OH** with the most intense peak (rt = 15.06 min).

chromatography with the highest content of the minor product **2β,15β-di-OH** yielded 12 mg (~0.5 %), as it was a mixture with the mono-hydroxylated compound **15β-OH** and the di-hydroxylated compound **7β,15β-di-OH**. This fraction was then subjected to purification by TLC, resulting in 1.1 mg of the pure compound. Therefore, it can be stated that the yield obtained from the TLC isolation process of the minor compound was 9.16 %.

2.3. Identification of functional groups of the compound 2β,15β-di-OH by FT-IR

The FT-IR spectrum I (film) obtained for the **2β,15β-di-OH** product is shown in **SM-S3.** Characteristic absorption bands corresponding to the functional groups present in the molecule were observed. In the region of 3447 cm^{-1}, the bands are attributed to the axial deformations or symmetric and asymmetric stretching vibrations of the hydroxyl groups (2β,15β) with hydrogen bonding. In the regions of 1676 cm^{-1} and 1728 cm^{-1}, bands correspond to the symmetric and asymmetric stretching of the C═O bonds of the carbonyl groups at C-3 (conjugated system) and C-20, respectively. The two bands present between 2923 and 2851 cm^{-1} are related to the symmetric and asymmetric stretching of C–H bonds of sp^3 carbon atoms. A band at 1614 cm^{-1} was also observed, which could be attributed to the C═C stretching (C-4 and C-5) due to the conjugation system with the carbonyl (C═O) at C-3. In the region between 1118 and 1022 cm^{-1}, bands related to C–O stretching vibrations were observed, in addition to bands at 1454 and 1356 cm^{-1}, which may be assigned to O–H bending vibrations. The bands at 803 and 752 cm^{-1} provide information on angular deformations of the C–H bonds out of the plane [16].

2.4. Circular Polarized Light Deviation of the compound 2β,15β-di-OH by Polarimetry

(2S,8R,9S,10R,13S,14S,15R,17S)-17-acetyl-2,15-dihydroxy-10,13-dimethyl-1,2,6,7,8,9,10,11,12,13,14,15,16,17-tetradecahydro-3H-cyclopenta[a]phenanthren-3-one ***(2β,15β-di-OH):*** Experimental data: $[\alpha]_D^{23}$ +

63,2 (*c* 0.50, $CHCl_3$).

2.5. Characterization of the compound 2β,15β-di-OH by NMR

The 1D NMR spectra (^1H and ^{13}C), their expansions, and the assignments of chemical shift values (δ), multiplicities (J) in Hertz (Hz) for **2β,15β-dihydroxyprogesterone**, are shown in Figs. 4 and 5, **SM-S4** and **SM-S5**, and in Tables 1 and 2 and Tables **SM-TS2** and **SM-TS3**.

The results of the 1D NMR analyses for the isolated minor compound **2β,15β-di-OH** were compared with the data for the major compounds previously obtained by de Paula et al. (2021).

It can be observed in Tables 1 and 2 that the δ values obtained for the signals of hydrogens and carbons for all compounds were generally similar. Notably, in the ^1H NMR spectrum for the compound **2β,15β-di-OH**, a singlet signal at $\delta = 5.83$ ppm corresponding to the hydrogen H-4 of the olefin was observed, with the area integration indicating 1 proton. Subsequently, peaks were observed at $\delta = 0.94$, 1.25, and 2.16, with integrals indicating the presence of 3H each, attributed to the methyl groups Me-18, Me-19, and Me-21, respectively. These results are in agreement with the data obtained for the compounds elucidated by de Paula et al. (2021). It is noteworthy that the signal for hydrogen H-2β was absent in the compound **2β,15β-di-OH** due to the presence of the hydroxyl group at this position, which was confirmed by the data from the 2D NMR spectra, FT-IR, and X-ray diffraction. Additionally, the signal for H-2α, typical of a carbinolic hydrogen, was observed with a chemical shift value at 4.20 ppm (dd, $J = 5.6$ and 13.9 Hz).

Regarding the ^{13}C NMR spectrum, a signal at $\delta = 199.6$ corresponding to the conjugated carbonyl carbon C-3 was observed. Additionally, signals at $\delta = 118.8$ and 174.8 were attributed to the olefinic carbons C-4 and C-5, respectively. Noteworthy results were found in the region typical for carbinolic carbons, with chemical shift values at 68.5 ppm (C-2) and 70.4 ppm (C-15). It should be highlighted that, in the major compounds **7β,15β-di-OH** and **15β-OH**, the typical signal for carbon C-2 appeared at $\delta = 33.9$ due to the absence of the hydroxyl group at this position. The signal for the methyl carbon C-19 showed a downfield shift due to the deshielding effect from the proximity of the hydroxyl group at carbon C-2. For the compound **2β,15β-di-OH**, the signal in the ^{13}C NMR spectrum appeared at 29.7 ppm, while for the compounds **7β,15β-di-OH** and **15β-OH**, the signals appeared at 17.3 and 17.9 ppm, respectively.

The 2D NMR HSQC spectrum for the compound **2β,15β-di-OH** is shown in **SM-S6**. Correlations were observed between the signals of several carbons and their respective hydrogens. Notably, for the carbinolic hydrogens, correlations were observed between H-2α and C-2 at 4.21 ppm and 68.5 ppm, respectively; and between H-15α and C-15 at 4.29 ppm and 70.4 ppm, respectively.

The 2D NMR HMBC spectrum for the **2β,15β-di-OH** compound is shown in **SM-S7**. Correlations between carbons and hydrogens (^2J, ^3J, and ^4J) were observed, confirming the positions of the hydroxylations at carbons C-2 and C-15. For the hydroxylation at C-2, correlations were observed between H-2α and C-3 (4.22 ppm–199.6 ppm), as well as with C-1 (4.22 ppm–39.5 ppm), as shown in Fig. 6(A). Additionally, correlations involving C-2 were observed: H-1α – C-2 (1.58 ppm–68.6 ppm), H-1β – C-2 (2.51 ppm–68.6 ppm), H-4 – C-2 (5.84 ppm–68.6 ppm), and Me-19 – C-2 (1.22 ppm–68.6 ppm), Fig. 6(B). Regarding the hydroxylation at C-15, correlations were observed between H-15α and C-13 (4.30 ppm–44.1 ppm) and with C-17 (4.30 ppm–63.7 ppm), Fig. 6(C). Correlations involving C-15 were observed, such as: H-14α – C-15 (1.08 ppm–70.5 ppm), H-16α – C-15 (2.21 ppm–70.5 ppm), and H-16β – C-15 (2.25 ppm–70.5 ppm), Fig. 6(D). It is noteworthy that the correlations involving H-15α and C-15 observed in the HMBC analysis for the **2β,15β-di-OH** compound were also described by de Paula et al. (2021) for the steroids **7β,15β-di-OH** and **15β-OH**, as all these compounds share the hydroxylation at C-15. The correlations observed from the HMBC analysis for the steroid **2β,15β-di-OH**, which confirmed the hydroxylations at carbons C-2 and C-15, are shown in Fig. 6(A–D).

From the 2D COSY NMR spectrum, correlations between ^1H–^1H nuclei, within a distance of up to ^3J, were observed (**SM-S8**). These analyses complemented those performed by HMBC for the **2β,15β-di-OH** steroid. Notable are the correlation signals presented by the hydroxylated hydrogen atoms attached to carbons C-2 and C-15 (Fig. 7). For H-2α ($\delta = 4.21$), correlations with H-1α ($\delta = 1.61$) and H-1β ($\delta = 2.50$) were observed, as shown in Fig. 7(A). For H-15α ($\delta = 4.29$), correlations with H-14α ($\delta = 1.10$), H-16α ($\delta = 2.21$), and H-16β ($\delta = 2.28$)

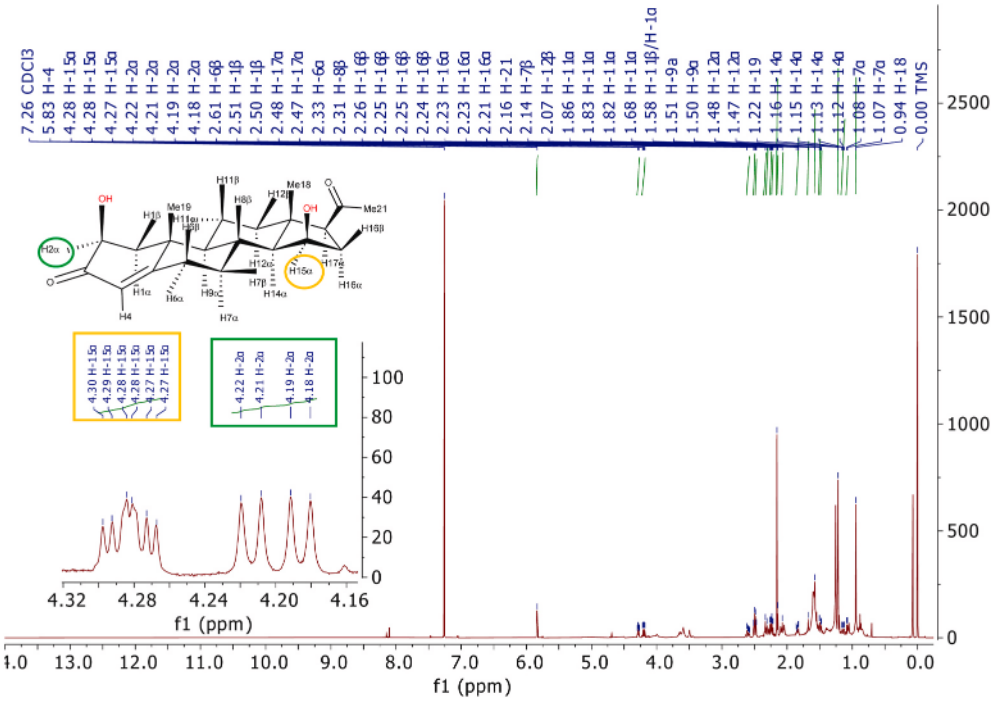

Fig. 4. ^1H NMR spectrum (500 MHz, $CDCl_3$) and its expansion in the region from 4.16 to 4.32 ppm of the **2β,15β-dihydroxyprogesterone** product. Highlighted in color are the hydroxylated positions (C-2 and C-15).

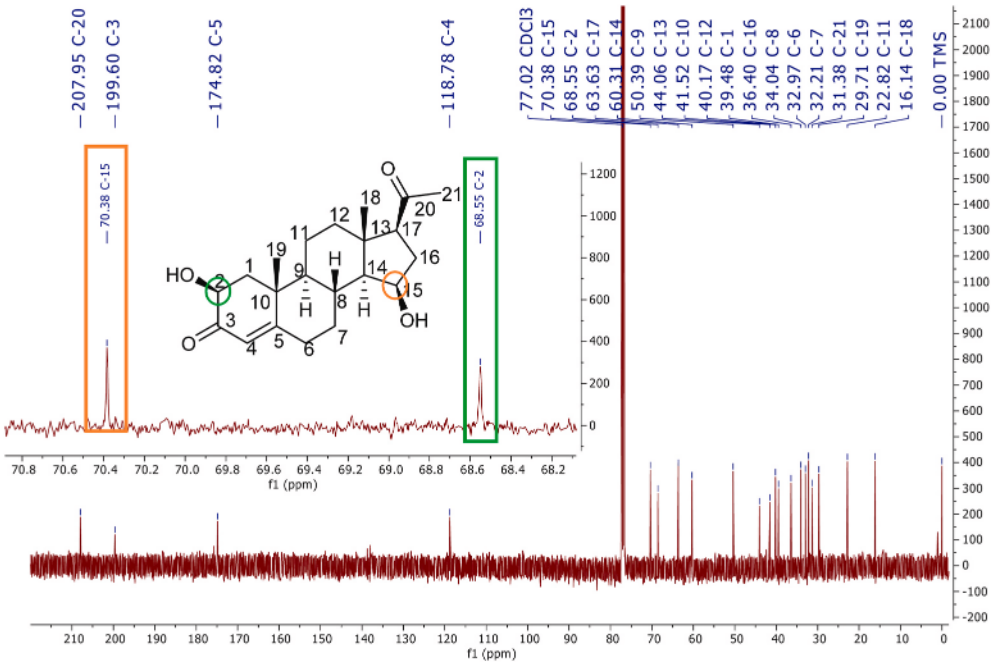

Fig. 5. ^{13}C NMR spectrum (125 MHz, $CDCl_3$) of the **2β,15β-dihydroxyprogesterone** product. Highlighted in color are the hydroxylated positions (C-2 and C-15).

Table 1
^{1}H NMR data (500 MHz, $CDCl_3$) for 2β,15β-dihydroxyprogesterone obtained experimentally, and for 15β-hydroxyprogesterone and 7β,15β-dihydroxyprogesterone obtained from the literature by De Paula et al. 2021[a].

Number IUPAC/ IUBMB	δ_H (ppm) 15β-OH	δ_H (ppm) 7β,15β-di-OH	δ_H (ppm) 2β,15β-di-OH
	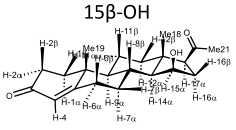	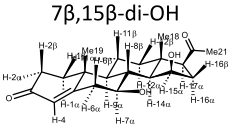	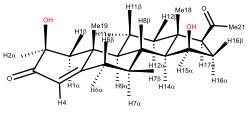

Table 2
^{13}C NMR data (125 MHz, $CDCl_3$) for **2β,15β-di-hydroxyrogesterone** obtained experimentally, and for 15β-hydroxyprogesterone and **7β,15β-dihydroxyprogesterone** obtained from the literature by De Paula et al. 2021[a].

Number IUPAC/ IUBMB	δ_C (ppm) **15β-OH**	δ_C (ppm) **7β,15β-di-OH**	δ_C (ppm) **2β,15β-di-OH**
	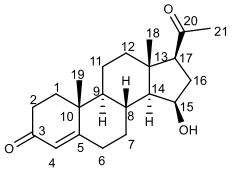	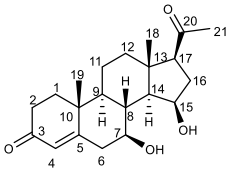	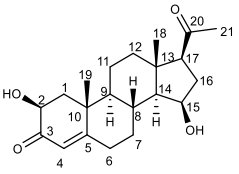

were observed, which were also described by De Paula et al. (2021) for the **7β,15β-di-OH** and **15β-OH** compounds. Thus, the correlations obtained from the COSY analyses for the **2β,15β-di-OH** compound further confirmed the hydroxylations at carbons C-2 and C-15.

From the 2D NOESY NMR spectrum, correlations between spatially proximate ^{1}H–^{1}H nuclei along the molecule were observed (**SM-S9**). Regarding the correlations observed for the carbinolic hydrogens, for H-2α ($\delta = 4.21$), correlations were observed with H-1α ($\delta = 1.61$), H-1β ($\delta = 2.50$), and H-9α ($\delta = 1.51$), as illustrated in Fig. 8(A).

Although the hydrogens H-2α and H-1β have distinct spatial orientations, the correlation between them observed in the NOESY spectrum is possible. As shown in the Newman projection for the steroidal ring "A" in Fig. 8(B), these hydrogens are spatially close to each other without steric hindrance, which explains the observed correlation.

For H-15α ($\delta = 4.29$), correlations were observed with H-6α and H-8β, whose signals overlap at $\delta = 2.33$. In the NOESY spectrum, correlations of H-15α with H-16α ($\delta = 2.21$), H-16β ($\delta = 2.28$), and H-7α ($\delta = 1.08$) were also observed. These observed correlations are consistent with the spatial "β" assignment of the hydroxyl groups located on carbons C-2 and C-15.

Through the analysis of the signal multiplicity in the ^{1}H NMR spectrum, it was observed that due to the different spatial orientations of the

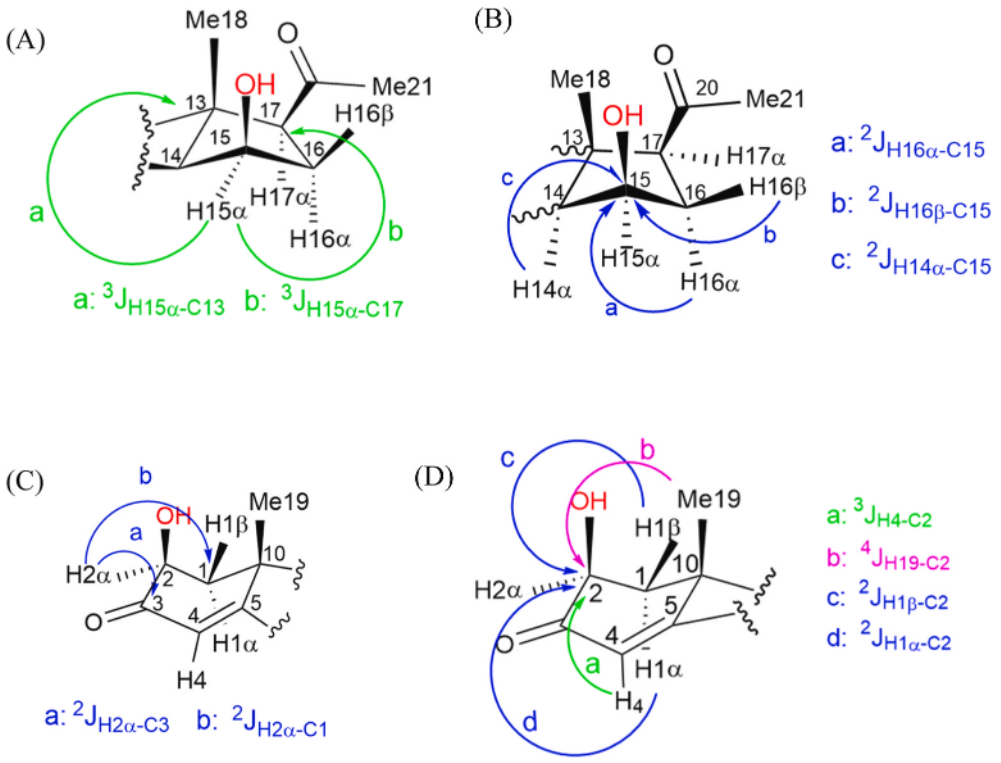

Fig. 6. $^1H–^{13}C$ correlations from the HMBC NMR spectrum (500 MHz, $CDCl_3$) for the compound **2β,15β-di-OH**. (A) Correlations observed with respect to hydrogen H-2α. (B) Correlations observed with respect to carbon C-2. (C) Correlations observed with respect to hydrogen H-15α. (D) Correlations observed with respect to carbon C-15.

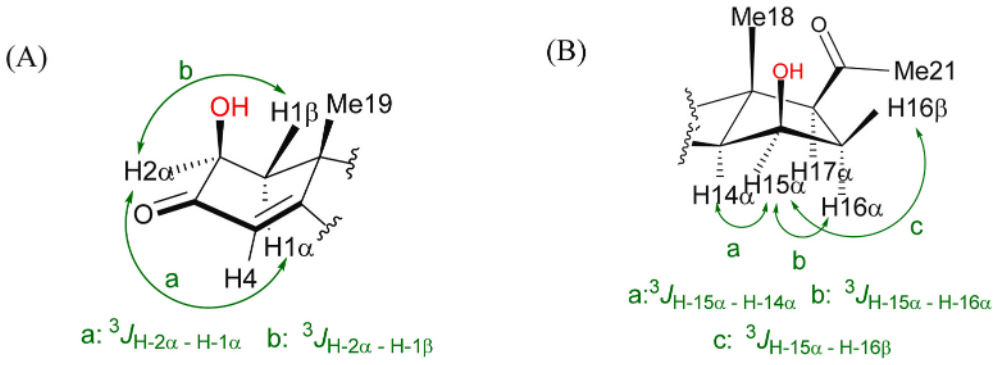

Fig. 7. Correlations observed in the $^1H–^1H$–COSY NMR spectrum (500 MHz, $CDCl_3$) for the compound **2β,15β-OHP**. (A) Correlations observed between H-2β-H-1α and H-2β-H-1β. (B) Correlations observed between H-15α-H-14α, H-15α-H-16α, and H-15α-H-16β.

protons H-1α and H-1β, these appear chemically distinct, splitting the signal for H-2α in the ^1H NMR spectrum into a doublet of doublets (dd). The calculated coupling constants were $J = 5.6$ and 13.9 Hz. The first value (5.6 Hz) was associated with the equatorial-equatorial interaction between protons H-2α and H-1β, while the 13.9 Hz value refers to the equatorial-axial interaction between protons H-2α and H-1α (Fig. 9(A)).

Regarding proton H-15α, the multiplicity of the signals of protons H-16β and H-14α was evaluated, as the signal for H-15α appeared as a multiplet. For H-16β, its relative configuration was evaluated as a doublet of doublets, with coupling constants of $J = 6.6$ Hz, related to the geminal interaction H-16β – H-16α, and $J = 2.7$ Hz, related to the *trans*-interactions between vicinal protons H-16β – H-15α and H-16β – H-17α (Fig. 9(B)). For H-14α, its relative configuration was evaluated as a doublet of doublets, with calculated coupling constants of $J = 12.1$ Hz, related to axial-axial interactions between vicinal protons H-14α – H-8β, and $J = 4.7$ Hz, related to the *cis*-interaction between vicinal protons H-14α – H-15α (Fig. 9(C)).

Thus, the coupling constants obtained from the splitting of the signals for H-2α, H-14α, and H-16α supported the β-orientations of the hydroxyl groups attached to C-2 and C-15 of the steroid **2β,15β-di-OH**, as can be concluded from the data obtained from the NOESY 2D NMR analyses.

Studies have shown that the hydroxylated compounds resulting from the bio-oxidation of progesterone by the fungus *P. oxalicum* CBMAI 1996 exhibited lower lipophilicity, which reduces their bioaccumulation potential in the environment. Additionally, computational simulations using the ECOSAR 2.0 program (Ecological Structure Activity Relationships) from the EPA (United States – Environmental Protection Agency) revealed that the hydroxylated derivatives of progesterone (**15β-OH** and **7β,15β-di-OH**) displayed a significant reduction in both acute and chronic ecotoxic effects. The values demonstrated in the study indicated a reduction in acute ecotoxicity by 10 and 100 times compared to progesterone, for the compounds **15β-OH** and **7β,15β-di-OH**, respectively, with a similar trend observed for chronic effects.

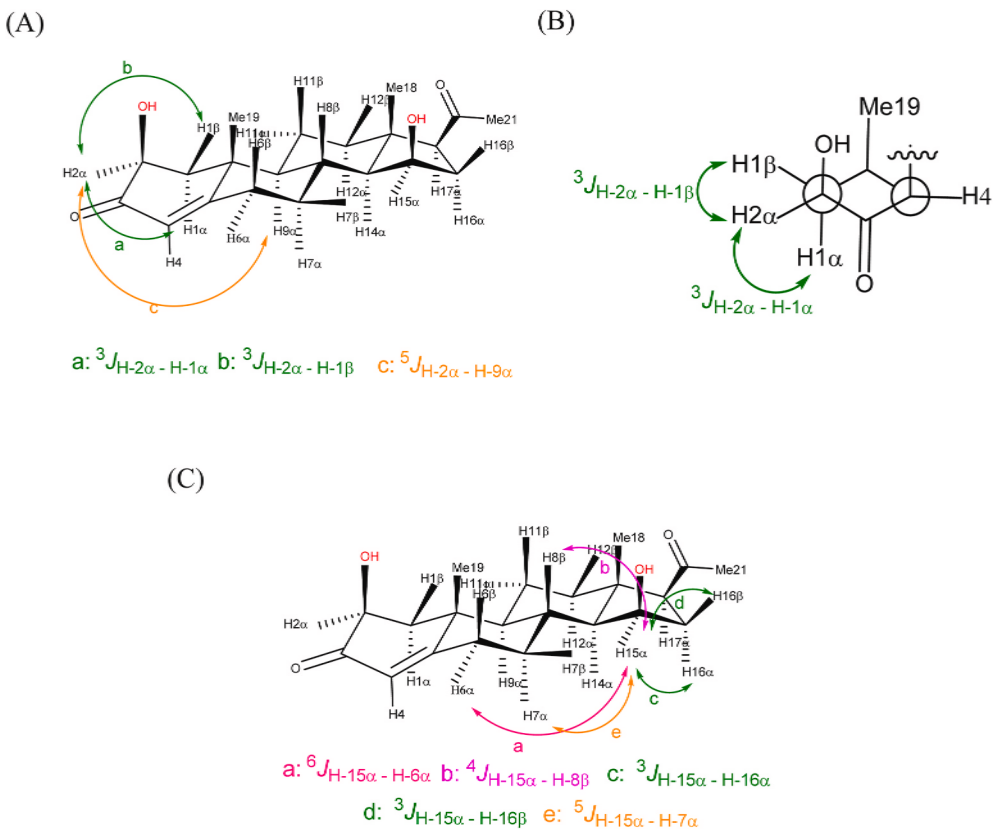

Fig. 8. Observed correlations in the NOESY NMR spectrum (500 MHz, $CDCl_3$) for the compound **2β,15β-di-OH**. (A) Correlations observed between H-2α – H-1α, H-2α – H-1β, and H-2α – H-9α. (B) Newman projection for the steroidal ring "A" highlighting the correlation H-2α – H-1β. (C) Correlations observed between H-15α – H-6α, H-15α – H-8β, H-15α – H-16α, H-15α – H-16β, and H-15α – H-7α.

Therefore, biotransformation studies are also crucial for the control and disposal of recalcitrant drugs, which can be emerging environmental contaminants [17].

2.6. X-ray diffraction characterization

The single crystal X-ray diffraction (SCXRD) allows the crystal structure determination, allowing the precise elucidation of atomic positions in the molecule, as well as the determination of the absolute configuration of stereogenic centers [18,19]. The single crystals obtained from the biotransformation products of progesterone, after the evaporation of the solvent used (ethyl acetate), were found suitable for X-ray analysis. In the present study, data from SCXRD of progesterone-derived compounds (**2β,15β-di-OH**, **15β-OH**, and **7β, 15β-di-OH**) were presented, offering a significant contribution. In addition to confirming the proposed structures, it allowed a comparison of the results with the assignments made by other characterization techniques. It is noteworthy that in the literature, the compounds **15β-OH** and **7β,15β-di-OH** have already been described, although the NMR spectral data were sometimes incomplete or inconclusive concerning the proposed structures.

SCXRD analyses revealed that di-hydroxylated compounds **2β,15β-di-OH** and **7β,15β-di-OH** crystallized in the monoclinic $P2_1$ and orthorhombic $P2_12_12_1$ space groups, respectively, with both presenting an asymmetric unit formed by a single molecule (Fig. 10(A) and B), with the structure of the product **7β,15β-di-OH** showing disorder in the C-11 and C-12 atoms, which were refined in two different positions with occupations of 50 %. Table **SM-ST4** presents some geometric parameters of the elucidated structures.

It was verified that in **2β,15β-di-OH** occurred the oxidation of carbons C-2 and C-15, where the hydroxyl groups are positioned in β-configuration, resulting in *S* and *R* configurations for carbons C-2 and C-15, respectively. For the **7β,15β-di-OH** product, the oxidation of the C-7 and C-15 carbons was verified, with the hydroxyls also in β-configuration, allowing an *S*-configuration for the C-7 carbon, while the C15 carbon is in an *R*-configuration. These results agree with the relative configurations proposed for these carbons by the nuclear magnetic resonance results.

In addition, it can be observed that in both structures the A and D rings have half-chair and envelope conformations, respectively, while the B and C rings are positioned in a chair configuration. The two structures present differences in the conformation of the A ring, where the positions of atoms C-1 and C-2 are inverted in relation to the plane formed by atoms C-3, C-4, C-5, and C-10 (Fig. 11). The conformation of the A-ring in the compound **2β,15β-di-OH** is different from the observed in the crystal structure of progesterone and most of its derivatives. However the same conformation was also observed in the structures of 6,19-epoxyprogesterone and 6,19-thioepoxyprogesterone [20].

A comparative analysis of the two dihydroxylated products **2β,15β-di-OH** and **7β,15β-di-OH**, highlights the distinct structural and conformational effects induced by hydroxylation at different positions of the steroidal framework. As shown in Fig. 11, hydroxylation at the C-2 position promotes a significant three-dimensional distortion of the A-ring, leading to a conformation that deviates from that typically observed for progesterone. In contrast, the A-ring conformation of the C-7–hydroxylated derivative remains similar to that of the progesterone scaffold.

These comparative structural differences are also evident in the spectroscopic data (previously discussed in Section 2.5), which reveal pronounced electronic effects associated with C-2 hydroxylation. In particular, the ^{13}C NMR chemical shift of C-2 is markedly deshielded in **2β,15β-di-OH** (δ = 68.5 ppm) compared to **7β,15β-di-OH** (δ = 33.9

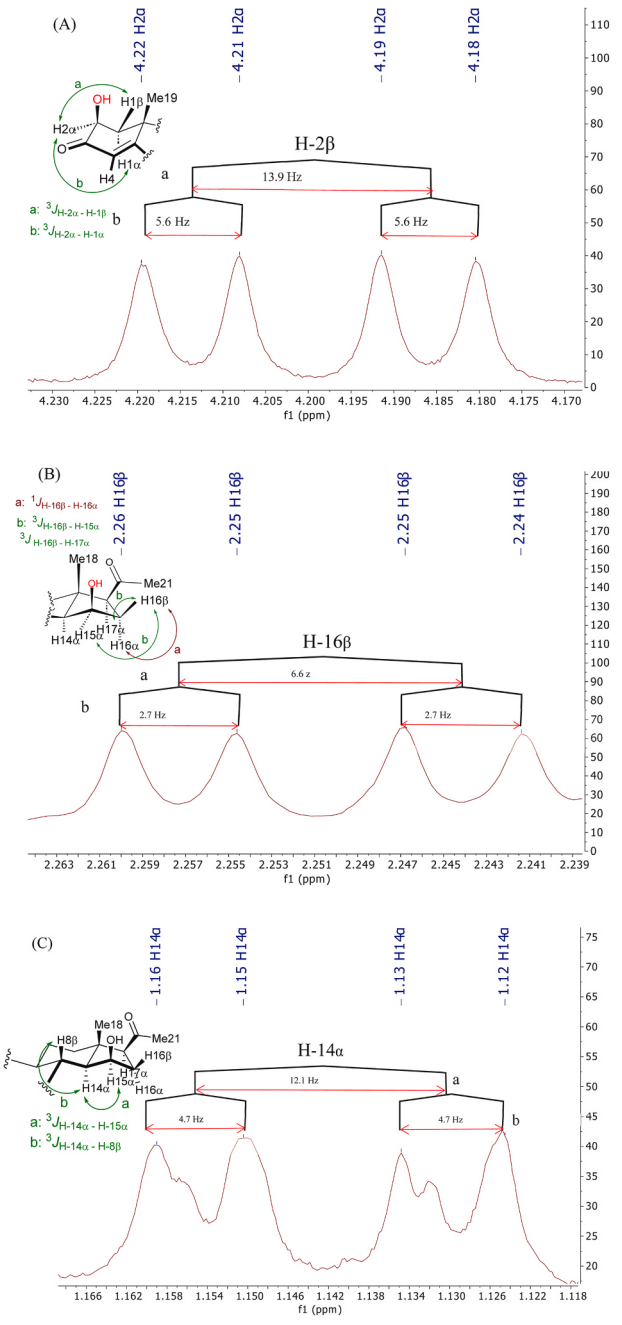

Fig. 9. Expansions of the ^{1}H NMR spectrum (500 MHz, $CDCl_3$) of the **2β,15β-di-hydroxyprogesterone** product in the region of: (A) 4.23–4.17 ppm; (B) 2.26–2.23 ppm; (C) 1.16–1.11 ppm.

ppm), accompanied by a corresponding downfield shift of the H-2 proton ($\delta = 4.20$ vs 2.38 ppm). Collectively, these observations demonstrate that hydroxylation at C-2 induces not only conformational but also significant electronic perturbations within the steroidal core, indicating that the enzymatic hydroxylation itself is responsible for generating pronounced chemical and electronic differentiation within the progesterone scaffold.

Single crystals of the mono-hydroxylated product **15β-OH** were also obtained, which crystallized in the monoclinic space group $P2_1$. The X-ray diffraction results showed that the product **15β-OH** crystallized with a quantity of **2β,15β-di-OH**, where it was initially verified a residual electron density near the carbon atom C-2 that corresponds to the presence of an oxygen atom, with an occupancy of 15 %, showing the obtaining of a mixture with 85 % of **15β-OH** and 15 % of **2β,15β-di-OH** (**SM-S10**). It was not possible to obtain pure crystals of **15β-OH** for this work, but the results obtained in the elucidated structure were enough for the determination of the absolute configuration and agree with the results obtained from the NMR analyses. Fig. 10(C) shows the asymmetric unit of the elucidated structure containing only the **15β-OH**, the component of the structure that will be discussed, while the representation of the asymmetrical unit containing the two components of the structure is found in the supplementary material.

For the mono-hydroxylated component of the structure, the bio-oxidation of C-15 carbon was confirmed with the insertion of hydroxyl group in the β-position, which resulted in obtaining the *R*-configuration for C-15 carbon. Regarding the rings present in the structure of the **15β-OH** product, it is observed that ring A is in a half-chair type conformation, as well as in the **7β,15β-di-OH** product, while rings B and C have a chair conformation, and ring D has an envelope conformation.

The structures of the three compounds obtained from the biotransformation of progesterone are stabilized by intermolecular O–H···O hydrogen bonds, as well as by intramolecular O–H···O interactions verified in the structures of the products **2β,15β-di-OH** and **7β,15β-di-OH** (Fig. SM–S11, **SM-S12** and **SM-S13; Table SM-TS5**). The presence of these non-covalent interactions allows the organization of the molecules of the obtained products into one-dimensional chains within their respective crystal lattices.

2.7. Hirshfeld surface analysis

For a better evaluation of the intermolecular interactions present in the crystal structures of the obtained products, the Hirshfeld Surfaces (HS) were generated for the compounds **2β,15β-di-OH** and **7β,15β-di-OH**, being mapped with the d_{norm} function. As the structure of the **15β-OH** has a mixture in its composition, its HS was not obtained. Fig. 12 shows the obtained surfaces.

The surfaces of both structures have intense red regions, which show the presence of intermolecular O–H···O hydrogen bonds, as discussed previously in X-ray diffraction analysis. In addition, two red regions in the surface of **2β,15β-di-OH** indicate a possible C═O···C interaction occurring between the oxygen atom O-1 of one molecule of **2β,15β-di-OH** with the carbon atom C-20 of a neighboring molecule, with O1···C20 distance of 2.903(3) Å.

By comparing the fingerprint plots (FPs) of the two compounds (Fig. SM–S14 and **SM-S15**), it is possible to observe that the positions of the hydroxyl groups and the conformation of the ring A resulted in FPs with different formats. Both FPs show that the H···H contacts are the most dominant in both structures (70.9 % in **2β,15β-di-OH** and 72.7 % in **7β,15β-di-OH**), with this high contribution explained by the large number of hydrogen atoms present in the molecular structures of **2β,15β-di-OH** and **7β,15β-di-OH**, mainly because they are in the most peripheral positions of the molecules. Two intense spikes in regions of lower values of d_i and d_e are verified in both FPs due to the presence of the O–H···O interactions, with the most intense spikes verified in the FP of **7β,15β-di-OH** because it presents stronger hydrogen bonds.

3. Conclusion

The present study demonstrated the efficient capacity of the marine fungus *P. oxalicum* CBMAI 1996 in the bio-oxidation of progesterone, resulting in mono- and di-hydroxylated products. The use of semi-preparative thin-layer chromatography proved to be effective in purifying the pre-fractionated extract from column chromatography, enabling the complete structural characterization of a new progesterone-derived product, **2β,15β-di-OH**.

Additionally, the crystals obtained at the end of the extract purification allowed for X-ray analysis of the compounds **15β-OH** and **7β,15β-di-OH**, which had been previously isolated and characterized by spectroscopic techniques (1D and 2D NMR, FTIR, HRMS). This confirmed the stereochemistry and the absolute configuration of these progesterone

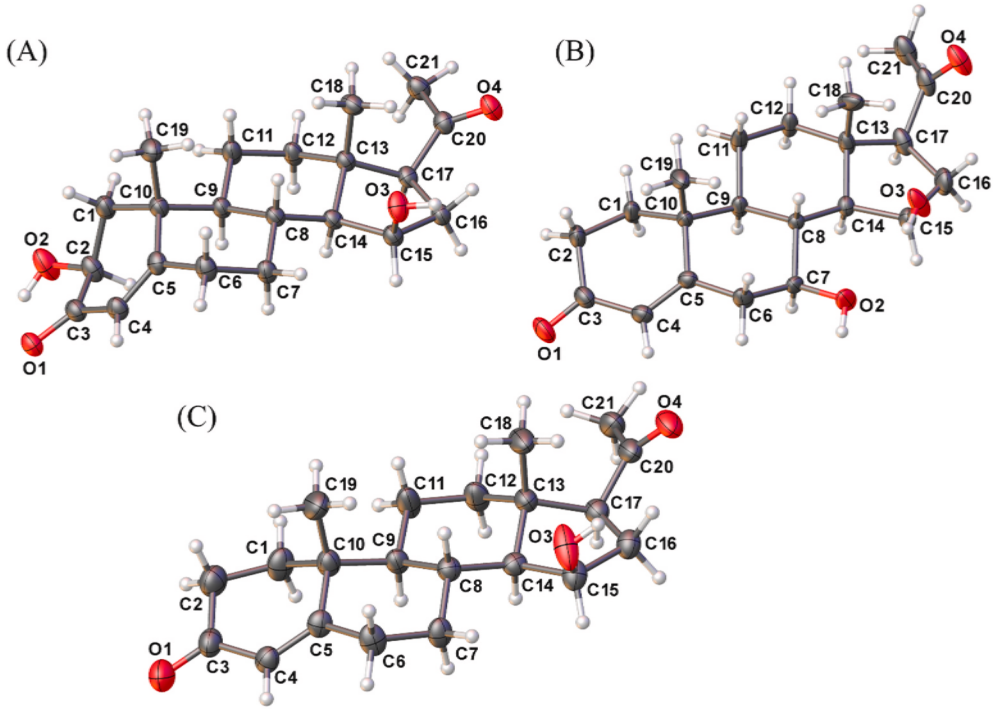

Fig. 10. ORTEP type illustrations of the asymmetric unities of (A) **2β,15β-di-OH** (B) **7β,15β-di-OH** and (C) **15β-OH**. Thermal ellipsoids represented at 50 % of probability level.

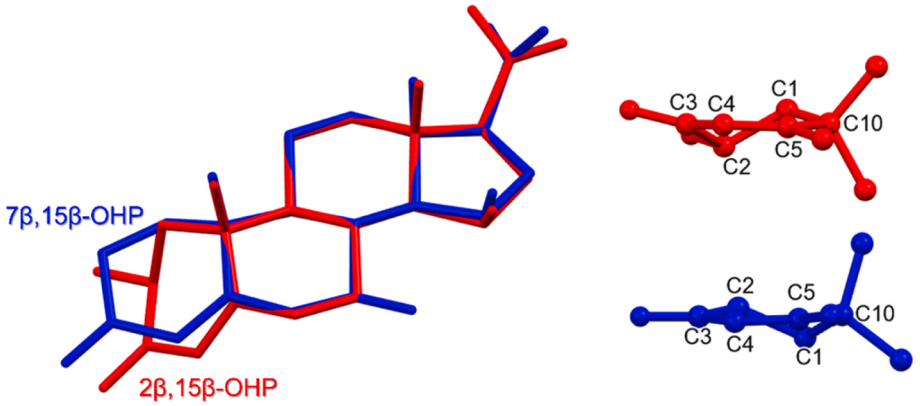

Fig. 11. Superposition of the structures of **2β,15β-di-OH** (red) and **7β,15β-di-OH** (blue), and visualization of their respective A rings.

steroidal derivatives at the carbon atoms that were bio-hydroxylated.

This work paves the way for future investigations into the application of these biotransformation processes in biotechnology, particularly concerning wastewater treatment for domestic use. The continuation of research may uncover additional aspects of the influence of these biological processes on the environment and their potential for the treatment of emerging steroidal pharmaceuticals that could act as bioaccumulators in the trophic chain.

4. Experimental Section

4.1. Biotransformation reaction of progesterone

The methodology employed in the biotransformation reaction of progesterone, as well as the preparation of the culture medium for obtaining biological material (mycelia and enzymatic broth) from the fungus *P. oxalicum* CBMAI 1996, the extraction procedures, and the purification of the compounds 2β,15β-di-OH, 7β,15β-di-OH, and 15β-OH, were reproduced following the protocols established by De Paula et al. (2021), as illustrated in Scheme 1. The biotransformation reaction was conducted using 50 mg of commercial progesterone (99 %) (acquired from Sigma-Aldrich) dissolved in 100 mL of fungal culture medium. In this present work, the biotransformation was conducted on a larger scale (more replicates) with the specific purpose of obtaining pure crystalline material for X-ray diffraction analysis. The increased mass of products obtained under these conditions enabled the identification and successful isolation of the novel minor derivative.

4.2. Isolation of the minor product 2β,15β-OHP by analytical thin layer chromatography (TLC)

Initially, an extract from the biotransformation reaction of progesterone, conducted in a reaction medium containing the fungal mycelial mass, was obtained following the protocol described by De Paula et al. (2021).

The crude extract (2.3 g), containing the progesterone

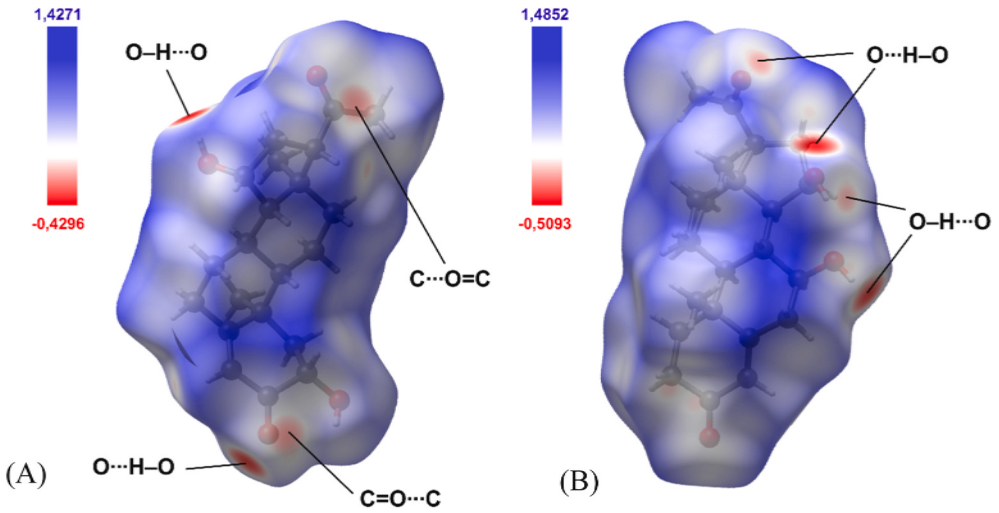

Fig. 12. Hirshfeld surfaces of (A) **2β,15β-di-OH** and (B) **7β,15β-di-OH**, mapped with d_{norm}.

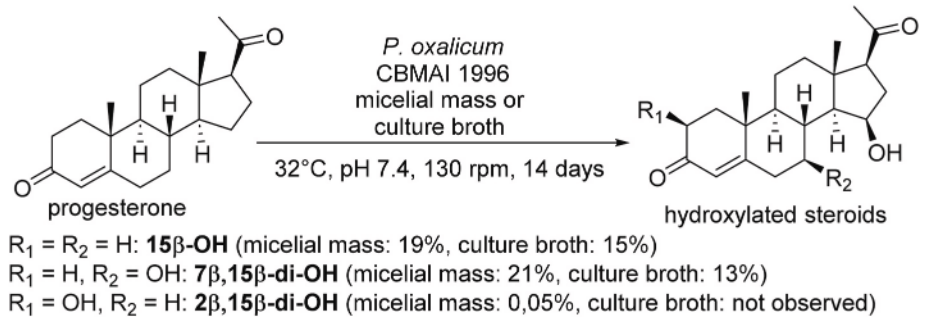

Scheme 1. Biotransformation reaction of progesterone by the mycelial mass or enzymatic broth of the fungus *P. oxalicum* CBMAI 1996.

biotransformation products of interest, was subjected to preliminary purification by column chromatography. The elution process commenced with a hexane/ethyl acetate solution (7:3) and was completed with pure ethyl acetate. The obtained fractions were subsequently analyzed by GC-MS (Section 2.3.1, Experimental Section).

Through this approach, it was possible to select the fractions from the column chromatography partitioning that contained a higher concentration of the compound **2β,15β-di-OH**. A total of 12 mg of the fraction with the highest product concentration was dissolved in chloroform and subjected to further purification using semi-preparative thin-layer chromatography (TLC) (DC-Fertigfolien POLYGRAM SIL G/UV254, 0.20 mm silica gel 60, fluorescent indicator UV254, 20 cm × 20 cm). The pre-purified extract solution containing the minor product **2β,15β-di-OH** was applied to an analytical TLC plate using a cotton swab, forming a 1 cm wide strip positioned 1 cm from the bottom edge. This procedure was repeated multiple times until the entire 12 mg sample, dissolved in chloroform, had been applied to a single TLC plate.

Next, 100 mL of the mobile phase solution, composed of 81 % dichloromethane, 14 % *n*-hexane, and 5 % methanol, was added to a glass chamber for thin-layer chromatography (TLC) (20 cm × 20 cm). The mobile phase composition was previously evaluated through analytical-scale tests using the same type of TLC plate. The chamber was sealed and allowed to stand for 20 min to saturate the internal atmosphere with solvent vapors. The TLC plate containing the sample was fixed onto a glass support using a clamp and then placed inside the chromatography chamber to promote component separation. The elution process lasted approximately 100 min (Supplementary Material, **SM-S16**).

After elution, the TLC plate was removed from the chamber, placed in a fume hood for solvent evaporation, and subsequently visualized under UV radiation at 254 nm. The product spots were observed as bands distributed along the plate, corresponding to their composition and purity relative to the biotransformation products (**SM-S17**). The regions on the plate were then marked with a pencil and carefully cut with scissors. The silica containing the adsorbed products corresponding to each selected fraction was scraped from the plate using a spatula and transferred to a beaker. Ethyl acetate was added to the beaker to promote dissolution and extraction of the biotransformation products. To enhance compound extraction, the mixture was subjected to vigorous stirring on a magnetic stirrer for 30 min. A simple filtration was then performed to remove the silica. The solvent was removed using a rotary evaporator, and samples from each fraction (corresponding to each excised plate region) were analyzed by GC-MS.

After solvent evaporation at room temperature, the sample containing the **2β,15β-di-OH** product crystallized (~1.1 mg), enabling subsequent structural characterization analyses, including NMR, FTIR, and X-ray diffraction.

4.3. Analyses for compound characterization

4.3.1. Gas chromatography coupled with mass Spectroscopy (GC-MS)

The Gas Chromatography-Mass Spectrometry analyses were performed using the Shimadzu GC2010 equipment, with the Shimadzu/AOC-5000 automatic sampler, Shimadzu MS2010 mass detector in ionization mode (EI, 70 eV), and an oven with a DB-5 J&W Scientific column (30 m × 0.25 mm x 0.25 μm). Helium flow: 6.6 mL min^{-1}, injector temperature: 250 °C, split ratio 1:5, initial temperature: 120 °C for 1 min, heating rate: 20 °C.min^{-1} for 9 min, 300 °C for 15 min, pressure 73.8 kPa, linear speed 36.1 cm s^{-1}, analysis time: 25 min. Mass spectra were obtained by a quadrupole analyzer filtering fragments of

m/z from 40 to 500, operating at 200 °C in the ion source and at 270 °C at the interface.

4.3.2. Fourier Transform Infrared Spectroscopy (FT-IR)

The FT-IR analysis was performed by dissolving the **2β,15β-di-OH** sample in chloroform ($CHCl_3$), which was then dropped onto a cell of a portable spectrometer from the brand Bruker, model Alpha ECO-ATR (ZnSe). After evaporation of the solvent at room temperature, the spectra were obtained in the range of 450–4000 cm^{-1}.

4.3.3. Optical rotation

The optical rotation was measured in $CHCl_3$ in a Jasco – Model P-2000 polarimeter equipped with a Na-lamp ($\lambda = 589$ nm), a 1.0 cm cuvette and 1.0 mL volume of solution at 23 °C. The concentration of the sample was 1.1 mg. mL^{-1}.

4.3.4. Nuclear magnetic resonance (NMR)

The NMR spectra (1D: ^{1}H, ^{13}C, and 2D: COSY, HSQC, HMBC and NOESY) of compounds **2β,15β-di-OH**, **15β-OH** and **7β,15β-di-OH** were recorded on Agilent Technologies 500/54 Premium Shielded (^{1}H NMR at 500 MHZ and ^{13}C NMR at 125 MHz).

A sample of **2β,15β-OHP** (1,0 mg) was prepared using $CDCl_3$ (1.0 mL) as solvent and TMS as internal standard. The chemical shifts were 0–15 ppm for ^{1}H and 0–230 ppm for ^{13}C. The coupling constants (*J*) were given in Hz. The 2D NOESY spectra was performed using a mixing time $\tau_m = 500$ ms.

FTIR, NMR, HRMS and optical rotation analyses were performed in Central de Análises Químicas Instrumentais (CAQI) from Instituto de Química de São Carlos – Universidade de São Paulo (IQSC-USP).

4.3.5. Single-crystal X-ray diffraction (SCXRD)

The single crystal X-ray diffraction measurements were executed at 100 K on a Rigaku XtaLAB Synergy-S diffractometer, equipped with a HyPix-6000HE detector and using a Cu Kα (1.54184 Å) radiation. CrysAlisPro [21] was used for cell refinement, as well as for data collection, data reduction and absorption correction. The structures were solved through the intrinsic phasing method from the SHELXT program [22], and refined using the least square methods of the SHELXL program [22], both within Olex2 program [23]. The non-hydrogen atoms were refined anisotropically, while the hydrogen atoms were refined in idealized positions, considering the geometry and hybridization of the atoms to which they are bonded. The figures of the structures and intermolecular interactions were generated using the Olex2 or the Mercury softwares [24]. Table **SM-ST1** presents some information about data collection and refinement of the structures.

The CIF files of the structures **2β,15β-di-OH**, **7β,15β-di-OH** and **15β-OH** were deposited in the *Cambridge Structural Database*, with CCDC codes 2416491, 2416492 e 2416493, respectively. The crystallographic data can be obtained free of charge in http://www.ccdc.cam.ac.uk/conts/retrieving.html.

4.3.6. Hirshfeld surface

Hirshfeld surfaces for dihydroxylated products **2β,15β-OHP** and **7β,15β-OHP** and their respective two-dimensional fingerprint plots (FP) were generated from the CIF files, using the CrystalExplorer 17.5 program [25], in order to investigate the intermolecular interactions present in the elucidated structures. The surfaces were mapped using the d_{norm} function, which is achieved by normalizing the functions d_i and d_e with respect to the van der Waals radii and has a color scheme to indicate the contacts smaller (red) and larger (blue) than the sum of the van der Waals radii of the atoms involved. The FP were obtained from the combination of the distances d_i and of being generated on a scale of 0.4–3.0 Å [26]. The Hirshfeld surface and the FP of the monohydroxylated compound **15β-OH**, since it was not possible to obtain pure single crystals.

CRediT authorship contribution statement

Ligia Breda e Vasconcelos: Writing – original draft, Project administration, Methodology, Investigation, Data curation. **Samuel Filipe Cardoso de Paula:** Writing – review & editing, Methodology, Data curation. **Pedro Henrique de Oliveira Santiago:** Writing – original draft, Software, Methodology, Data curation. **Javier Ellena:** Writing – review & editing, Supervision. **André Luiz Meleiro Porto:** Writing – review & editing, Project administration.

Declaration of competing interest

The authors declare that they have no known competing financial interests or personal relationships that could have appeared to influence the work reported in this paper.

Acknowledgements

The authors thank the University of São Paulo (USP) and the São Carlos Chemistry Institute (IQSC) for the infrastructure to develop the project. LBV thanks the São Paulo Research Foundation (FAPESP) (Proc. N0. 2021/13179-5) for the scholarship. PHOS thanks to São Paulo Research Foundation (FAPESP) (Proc. N°. 2021/10066-5). JE thanks to São Paulo Research Foundation (FAPESP) (Proc. N°. 2017/15850-0 and 2021/02522-0) and National Council for Scientific and Technological Development (CNPq) (Proc. N°. 312505/2021-3). ALMP thanks the National Council for Scientific and Technological Development (CNPq) (Proc. N°0.131225/2022-7). ALMP thanks the São Paulo Research Foundation (FAPESP) (Proc. 2016/20155-7) for financial resources for research development.

Appendix A. Supplementary data

Supplementary data to this article can be found online at https://doi.org/10.1016/j.tet.2026.135150.

Data availability

Data will be made available on request.

References

During the preparation of this work the authors used Chat GPT service in order to review and improve the translation of the text. After using this tool, the authors reviewed and edited the content as needed and takes full responsibility for the content of the published article.

[1] G.-G. Ying, R.S. Kookana, Y.-J. Ru, Occurrence and fate of hormone steroids in the environment, Environ. Int. 28 (2002) 545–551, https://doi.org/10.1016/S0160-4120(02)00075-2.
[2] J.A.R. Salvador, M.M.C. Silva (Eds.), Chemistry and Biological Activity of Steroids, 2020, https://doi.org/10.5772/intechopen.77331.
[3] N.M. Kassab, Determinação De Hormônios Esteróides Em Contraceptivos Orais Por Cromatografia Líquida De Alta Eficiência (CLAE), University of São Paulo, 2001.
[4] Z.-M. Li, K. Kannan, Determination of 19 steroid hormones in human serum and urine using liquid chromatography-tandem mass spectrometry, Toxics 10 (2022), https://doi.org/10.3390/toxics10110687.
[5] M. Md S. Yazdan, R. Kumar, S.W. Leung, The environmental and health impacts of steroids and hormones in wastewater effluent, as well as existing removal technologies: a review, Ecologies 3 (2022) 206–224, https://doi.org/10.3390/ecologies3020016.
[6] B. Almazrouei, D. Islayem, F. Alskafi, M.K. Catacutan, R. Amna, S. Nasrat, B. Sizirici, I. Yildiz, Steroid hormones in wastewater: sources, treatments, environmental risks, and regulations, Emerging Contam. 9 (2023) 100210, https://doi.org/10.1016/j.emcon.2023.100210.
[7] S.F.C. de Paula, Estudo Da Ocorrência De Reações De bio-oxidação Dos Esteroides Progesterona E 17(alfa)-etinil Estradiol Por Fungos De Ambiente Marinho, University of São Paulo, 2016.
[8] E.R. Olivera, J.M. Luengo, Steroids as environmental compounds recalcitrant to degradation: genetic mechanisms of bacterial biodegradation pathways, Genes 10 (2019), https://doi.org/10.3390/genes10070512.
[9] O.S. Savinova, P.N. Solyev, D.V. Vasina, T.V. Tyazhelova, T.V. Fedorova, T. S. Savinova, Biotransformation of progesterone by Aspergillus nidulans VKPM F-

1069 (wild type), Steroids 149 (2019) 108421, https://doi.org/10.1016/j.steroids.2019.05.013.
[10] E. Kozłowska, J. Sycz, T. Janeczko, Hydroxylation of progesterone and its derivatives by the entomopathogenic strain Isaria farinosa KCh KW1.1, Int. J. Mol. Sci. 23 (2022), https://doi.org/10.3390/ijms23137015.
[11] V.H.P. dos Santos, R.S. Andre, J.P. dos Anjos, L.A. Mercante, D.S. Correa, E. O. Silva, Biotransformation of progesterone by endophytic fungal cells immobilized on electrospun nanofibrous membrane, Folia Microbiol. 69 (2024) 407–414, https://doi.org/10.1007/s12223-023-01113-4.
[12] T.M. de Queiroz, T.A. Valdes, A. Leitão, A.L.M. Porto, Bio-oxidation of progesterone by Penicillium oxalicum CBMAI 1185 and evaluation of the cytotoxic activity, Steroids 205 (2024) 109392, https://doi.org/10.1016/j.steroids.2024.109392.
[13] S.F.C. de Paula, I.G. Rosset, A.L.M. Porto, Hydroxylated steroids in C-7 and C-15 positions from progesterone bio-oxidation by the marine-derived fungus Penicillium oxalicum CBMAI 1996, Biocatal. Agric. Biotechnol. 37 (2021) 102167, https://doi.org/10.1016/j.bcab.2021.102167.
[14] T.J. Cole, K.L. Short, S.B. Hooper, The science of steroids, Semin. Fetal Neonatal Med. 24 (2019) 170–175, https://doi.org/10.1016/j.siny.2019.05.005.
[15] R.A. Hill, H.L.J. Makin, D.N. Kirk, G.M. Murphy, Dictionary of Steroids, Taylor \& Francis, 1991.
[16] R.M. Silverstein, F.X. Webster, Identificação Espectrométrica De Compostos Orgânicos, sixth ed., LTC Livros Técnicos e Científicos, Rio de Janeiro, 2000.
[17] L.B. e Vasconcelos, S.F.C. de Paula, A.L.M. Porto, Estudos Recentes Da Biotransformação Da Progesterona Por Microrganismos, Ciências exatas e da terra: teorias e princípios 2 (2023) 77–101, https://doi.org/10.22533/at.ed.3742302085.
[18] R. Benassi, U. Folli, D. Iarossi, L. Schenetti, F. Taddei, A. Musatti, M. Nardelli, Conformational analysis of organic carbonyl compounds. Part 11. Conformational properties of difuryl, dithienyl, and furyl thienyl ketones studied by X-ray crystallography, n.m.r. lanthanide-induced shifts and ab-initio MO calculations, Journal of the Chemical Society, Perkin Transactions 2 (1989) 1741–1751, https://doi.org/10.1039/P29890001741.
[19] G.H. Stout, L.H. Jensen, X-Ray Structure Determination: a Practical Guide, Wiley, 1989.
[20] A.S. Veleiro, A. Pecci, M.C. Monteserín, R. Baggio, M.T. Garland, C.P. Lantos, G. Burton, 6,19-Sulfur-Bridged progesterone analogues with antiimmunosuppressive activity, J. Med. Chem. 48 (2005) 5675–5683, https://doi.org/10.1021/jm049266x.
[21] Oxford Diffraction/Agilent Technologies UK Ltd, CrysAlisPro, 2024.
[22] G.M. Sheldrick, SHELXT - integrated space-group and crystal-structure determination, Acta Crystallogr., Sect. A: Found. Crystallogr. 71 (2015) 3–8, https://doi.org/10.1107/S2053273314026370.
[23] O. V Dolomanov, L.J. Bourhis, R.J. Gildea, J.A.K. Howard, H. Puschmann, OLEX2: a complete structure solution, refinement and analysis program, J. Appl. Crystallogr. 42 (2009) 339–341, https://doi.org/10.1107/S0021889808042726.
[24] C.F. MacRae, I. Sovago, S.J. Cottrell, P.T.A. Galek, P. McCabe, E. Pidcock, M. Platings, G.P. Shields, J.S. Stevens, M. Towler, P.A. Wood, Mercury 4.0: from visualization to analysis, design and prediction, J. Appl. Crystallogr. 53 (2020) 226–235, https://doi.org/10.1107/S1600576719014092.
[25] M.J. Turner, J.J. McKinnon, S.K. Wolff, D.J. Grimwood, P.R. Spackman, D. Jayatilaka, M.A. Spackman, Crystalexplorer 17.5, 2017.
[26] M.A. Spackman, D. Jayatilaka, Hirshfeld surface analysis, CrystEngComm 11 (2009) 19–32, https://doi.org/10.1039/B818330A.